A FIELD STUDY OF DIFFUSION AROUND A MODEL CUBE IN A SUBURBAN AREA

SUSUMU OIKAWA and YAN MENG
Environmental Engineering Department, Institute of Technology, Shimizu Corporation, No. 4-17, Etchujima, 3-chome, Koto-ku, Tokyo 135, Japan

(Received in final form 8 January, 1997)

Abstract. To investigate diffusion around a building in a suburban area, a field observation was conducted on a model cube with a centrally located rooftop level source in September 1992 in Sapporo, Japan. The results show that high concentrations were observed both upwind and downwind of the source on the roof, although the mean velocity U was positive. The values of normalized concentration at locations upwind and downwind of the source were lower than those obtained from wind tunnel data conducted at moderated turbulence levels. At ground level, the mean concentrations along the model centre line show the highest value near the cube and decay rapidly in the downstream direction. The relationship between the instantaneous concentrations and instantaneous velocity was investigated using two fast-response concentration detectors and an ultrasonic anemometer. It was found that when reverse flow occurred on the roof, the tracer gas was detected upwind of the source.

1. Introduction

Over the last two decades, the mean concentration field around a building has often been studied in the wind tunnel. The effluent plume from a nearby stack becomes trapped in the cavity wake behind buildings. This phenomenon, known as 'downdraft', leads to a high concentration of pollutants at ground level. In relation to the concentration and flow on the roof of buildings, an early wind tunnel study was conducted by Halitsky (1963) on a cube model with a centrally located rooftop level source placed in a uniform flow. He inferred the existence of a reverse flow on the roof by measuring the concentration field. Wilson (1976) conducted a study on the flow around rectangular buildings in a thick boundary layer flow and found that the flow reattached to the roof, while Halitsky's study did not find reattachment. For effects of oncoming flow conditions, a systematic wind tunnel study was conducted by Ogawa et al. (1983a,b). They found that the change in the flow pattern on the roof due to differences in upwind turbulence caused the concentration patterns on the roof, as well as those behind the building, to change.

Although research on the mean concentration near buildings has been conducted not only through wind tunnel studies but also through a number of field studies conducted in flat terrain, (see, for example, Munn and Cole, 1967; Hinds, 1969; Drivas and Shair, 1974; Smith, 1975; Ogawa and Oikawa, 1982; Ogawa et al., 1983a,b; Jones and Griffiths, 1984; and Higson et al., 1994), little observation has been made of diffusion in an urban area, where the existence of high levels of turbulence has been reported (e.g., Bowne and Ball,1970; Jackson,1978; Uno et al.,1988; Rotach,1993; Oikawa and Meng, 1995).

Boundary-Layer Meteorology **84:** 399–410, 1997.

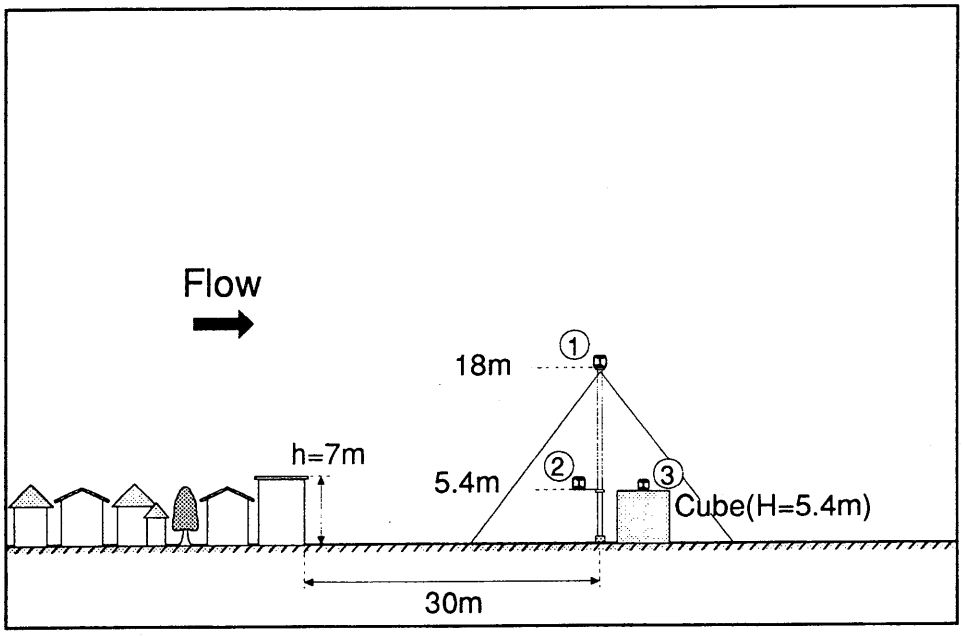

Figure 1. Schematic of the experiment setup. The ultrasonic anemometers (1) and (2) were upwind of the cube and (3) was set at the centre of the cube rooftop.

To clarify the diffusion phenomenon around a building in an urban area, a field study was conducted using several ultrasonic anemometer-thermometers and fast-response concentration detectors in Sapporo, Japan. This paper presents the results concerning (i) the mean concentration patterns on the rooftop of the model cube and at ground level, and (ii) the relationship between the instantaneous concentrations and instantaneous velocity found on the rooftop of the cube.

2. Observation Site and Experiment Setup

The field study was conducted in Sapporo, Japan, in September, 1992. The observation site was located 10 km northwest of the center of the city. Residential dwellings, which are uniformly seven metres high, are first noted 30 metres to the northwest of the site, and continue 2 km towards the coast. Details on the site can be found in Oikawa and Meng (1995). The model cube, which was made from plywood sheets with 5.4 m on each edge, was set back 30 m from the houses. Observations were conducted whenever the wind blew from the northwest. Figure 1 shows a schematic of the field site. The two three-dimensional ultrasonic anemometer-thermometers (Kaijo Corporation) were mounted at 5.4 m and 18 m on poles, and one two-dimensional ultrasonic anemometer was set at the center of the roof at 5.5 m. The sonic anemometers were calibrated in a wind tunnel.

In this study, two different tracer gases, Sulfur Hexafluoride (SF_6) and Ethylene (C_2H_4), were used. The two tracer gases were mixed with nitrogen and were released at a constant rate (70 l/min) from a 30 cm diameter source on the surface

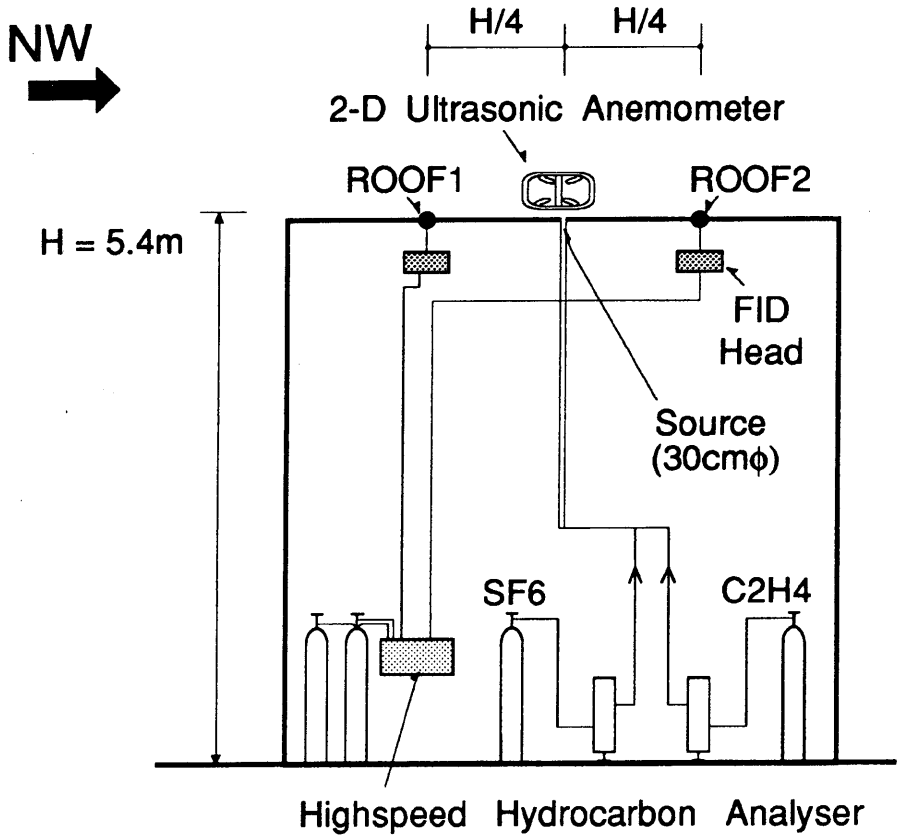

Figure 2. Tracer gas release system and fast-response concentration detector setup.

at the center of the roof. The exhaust velocity was about 1.6 cm s^{-1}, low enough to avoid any jet effect. SF_6 gas was used to obtain the average concentration. There were 50 sampling ports on the roof of the cube and near the ground. The sample gas was fed into bags at a sampling rate of 200 cc/min for 10 min; later, the sample gas was analyzed by an ECD gas chromatograph. C_2H_4 gas was used to obtain the concentration variations, and analyzed by flame-ionization detectors (FID) manufactured commercially (HFR-400 made by Cambustion Ltd of England). The sensors were 0.25 mm in diameter by 5 cm long. The response time, which is the time from when the gas started combusting in the FID head until the output reached 63% of steady value, was less than 0.02 s. Two sensors (ROOF1 and ROOF2 in Figure 2) were positioned on the roof. They were placed 1 cm above the roof and were calibrated before the start of each run. Calibration was done by intaking standard gases (0, 10, 40, 100, 400, 1000 ppm) via a teflon bag and a tube mounted at the top of the probe. The response of the detectors is linear to within ±5% over the operating range of 0–1000 ppm.

Data from both the sonic anemometers and the FIDs were collected on a digital recorder (TEAC Co., DR-F1) at a 10Hz sampling rate. This frequency was chosen to

Table I
Summary of the flow characteristics of the oncoming wind (at z = 5.4 m)

Run	U (m s^{-1})	σ_u (m s^{-1})	σ_v (m s^{-1})	σ_w (m s^{-1})	u_* (m s^{-1})	$\overline{w'\theta'}$ (m s^{-1} K)	L (m)	ϕ (deg)	σ_ϕ (deg)
1	1.8	0.70	0.57	0.32	0.25	0.02	−55	−5	20
6	1.3	0.64	0.64	0.30	0.27	0.03	−54	3	31
9	2.8	1.05	1.08	0.72	0.58	0.08	−167	8	23
10	2.3	1.18	0.97	0.68	0.59	0.06	−230	8	27
11	2.4	1.00	0.74	0.53	0.45	0.03	−191	−15	20
15	5.8	1.94	1.58	0.95	0.70	0.02	−1041	13	15

Table II
Comparison of the wind-tunnel data R6 (Ogawa et al., 1983a) and the field data Run 6 of the oncoming wind (at $z = H$)

	Case	σ_u/U	σ_v/U	σ_w/U
Wind tunnel	R6	0.265	0.237	0.224
Field	Run 6	0.492	0.492	0.230

be compatible with the response of the sonic anemometers. A 10-minute averaging time was used for each run.

In the present study, wind directions (ϕ), where ϕ is the wind direction measured from the plane perpendicular to the upwind face of the model, were selected within $\phi = \pm 15°$. A total of sixteen runs were conducted and six runs were within $\phi = \pm 15°$. Atmospheric conditions and turbulence properties during these runs are shown in Table I. Here, U is the mean horizontal wind speed, and σ_u, σ_v, and σ_w are the standard deviations of the fluctuating velocity components of the alongwind (x), crosswind (y), and vertical (z) directions, respectively. u_* is the friction velocity, which was derived from the eddy correlation measurements, with $u_* = \sqrt{-\overline{u'w'}}$, and L is the Monin–Obukhov length, $L = -u_*^3 T_0/\kappa g \overline{w'\theta'}$, where θ' is temperature fluctuation, κ is the von Karman constant (0.41), T_0 is the potential temperature, and g is the acceleration due to gravity. σ_ϕ is the standard deviation of the fluctuating wind direction. Observations were conducted mainly during the daytime on both clear and cloudy days. Atmospheric stabilities were slightly unstable, where the values of the Monin–Obukhov length (L) at z = 5.4 m ranged from −54 m to −1041 m.

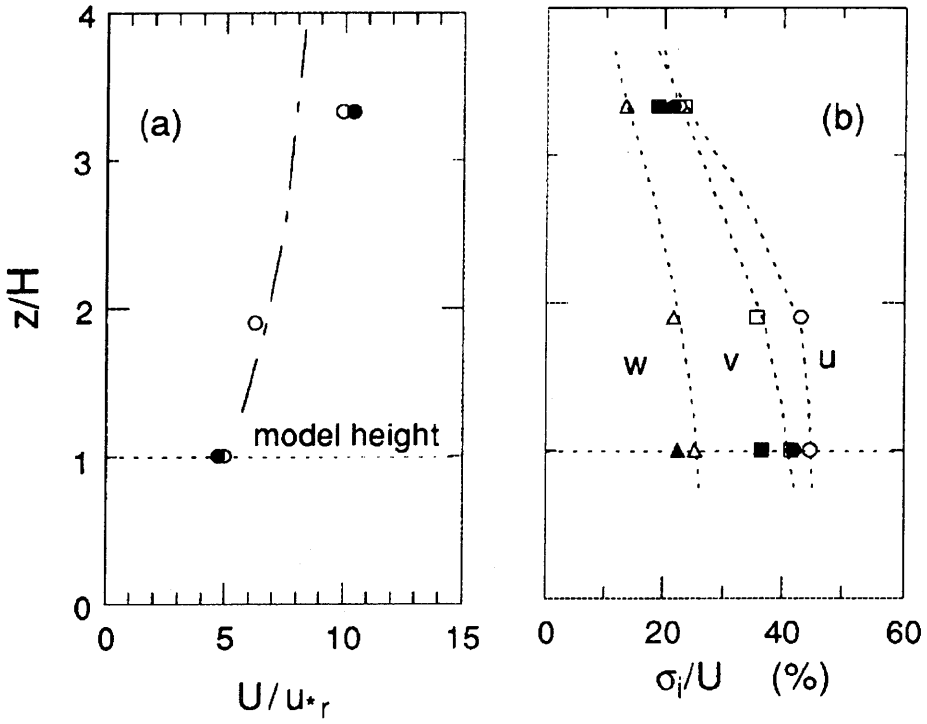

Figure 3. The profiles of (a) normalized mean wind velocity (b) σ_u/U, σ_v/U and σ_w/U. The unfilled symbols represent data observed in Nov. 1992 (Oikawa and Meng, 1995) and the filled symbols are data from the 6 runs in Table I. The dotted lines in (a) denote the mean wind profiles calculated by the equation $U/u_* = (1/\kappa)\{\ln(z'/z_0) - \psi(z'/L)\}$. In (b), the dashed curves were drawn by eye.

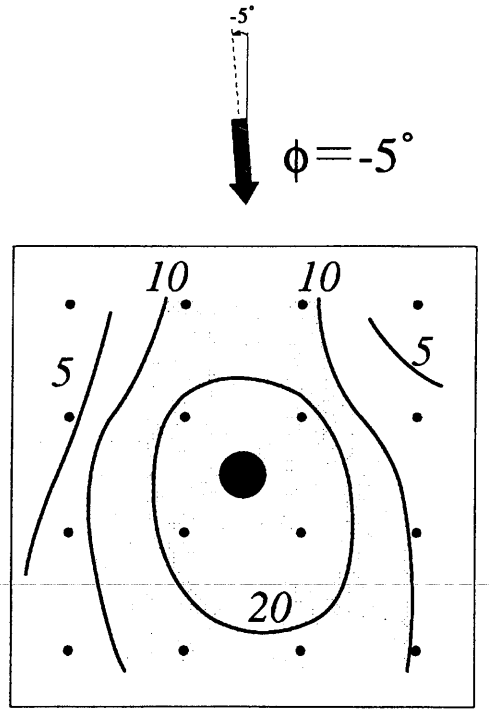

Figure 4. Normalized concentration patterns on the roof (Run 1).

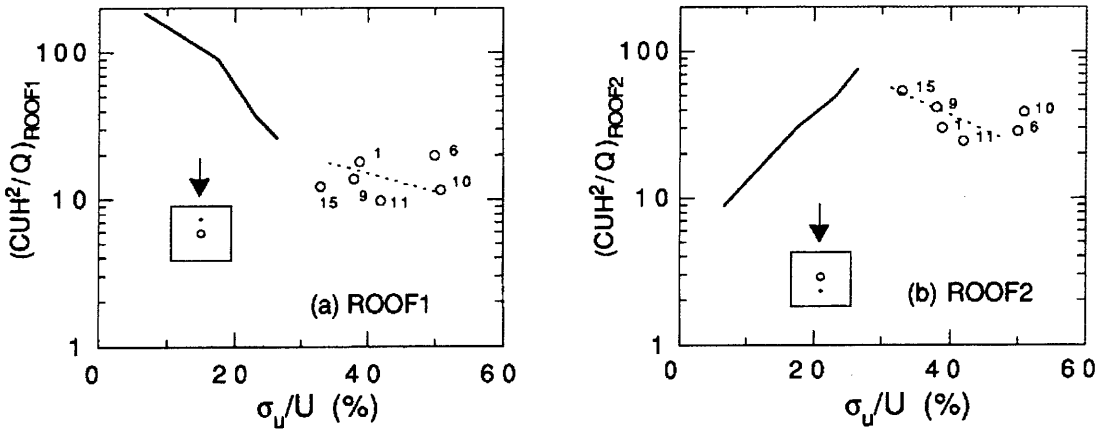

Figure 5. Normalized concentration vs σ_u/U. Solid lines indicate wind-tunnel data ($\phi = 0°$, after Ogawa et al., 1983b). Numbers represent run numbers. (a) ROOF1 (upwind), (b) ROOF2 (downwind).

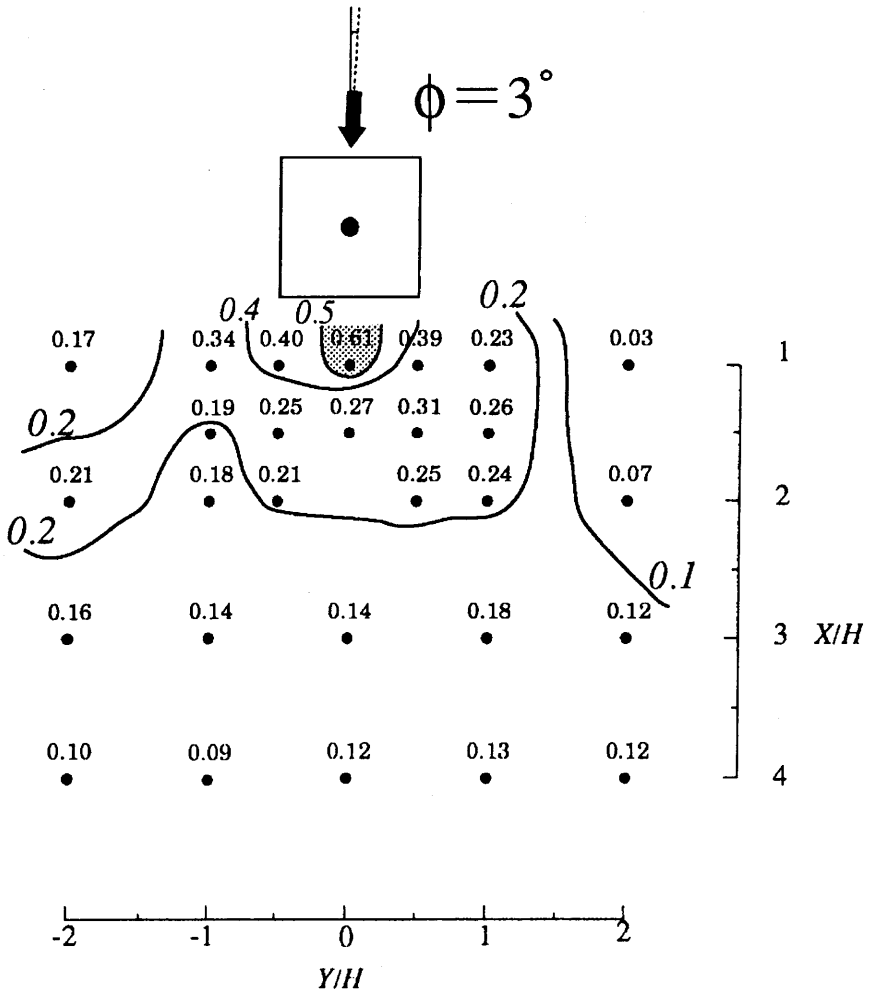

Figure 6. Normalized concentration patterns on the ground (Run 6).

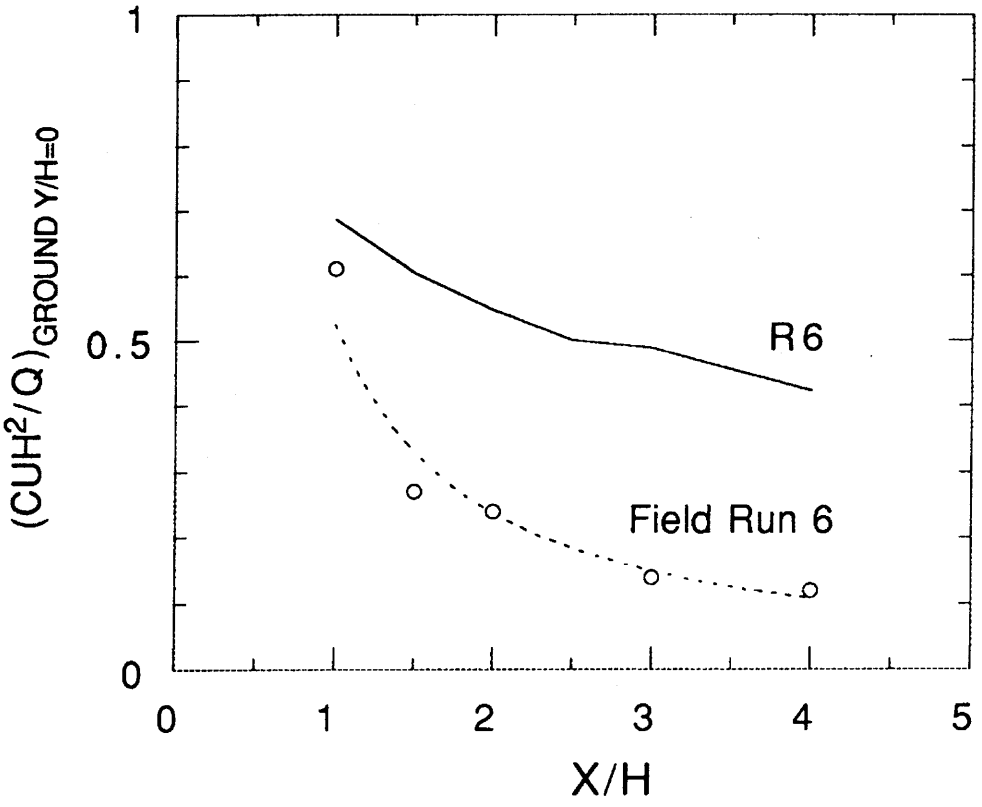

Figure 7. The normalized concentration along the cube centre line on the ground, wind-tunnel data R6 (after Ogawa et al., 1983b) and field data Run 6.

3. Results and Discussion

3.1. Vertical Profiles of Mean Velocity and Turbulence Intensity

Figure 3 (a) shows an example of the upwind mean wind speed profiles, plotted against normalized height z/H (H = 5.4 m, where H is the model cube height). The unfilled symbols represent data observed in Nov. 1992 (Oikawa and Meng, 1995) and the filled symbols are data from the 6 runs shown in Table I. The dotted line in Figure 3(a) represents non-neutral wind profiles calculated by the equation of $U/u_* = (1/\kappa)\{\ln(z'/z_0) - \psi(z'/L)\}$, where $\psi(z'/L)$ is the Monin–Obukhov function as described by Carl et al. (1973), z_0 is the roughness length (= 0.45 m) which is assessed using the method described by Lettau (1969), and L is the Monin–Obukhov length measured at z = 18 m. Here, z' is $z' = z - d$, where z is the height above ground, and d (= 2.3 m) is the zero-plane displacement, as calculated using the method described by Counihan (1971). The calculated wind profiles appear to display the same tendency as those found in the present study, although the observed value of U/u_* at z = 18 m was slightly larger than the calculated value. Figure 3(b) presents local turbulence intensity profiles of the three velocity components. The

(a)

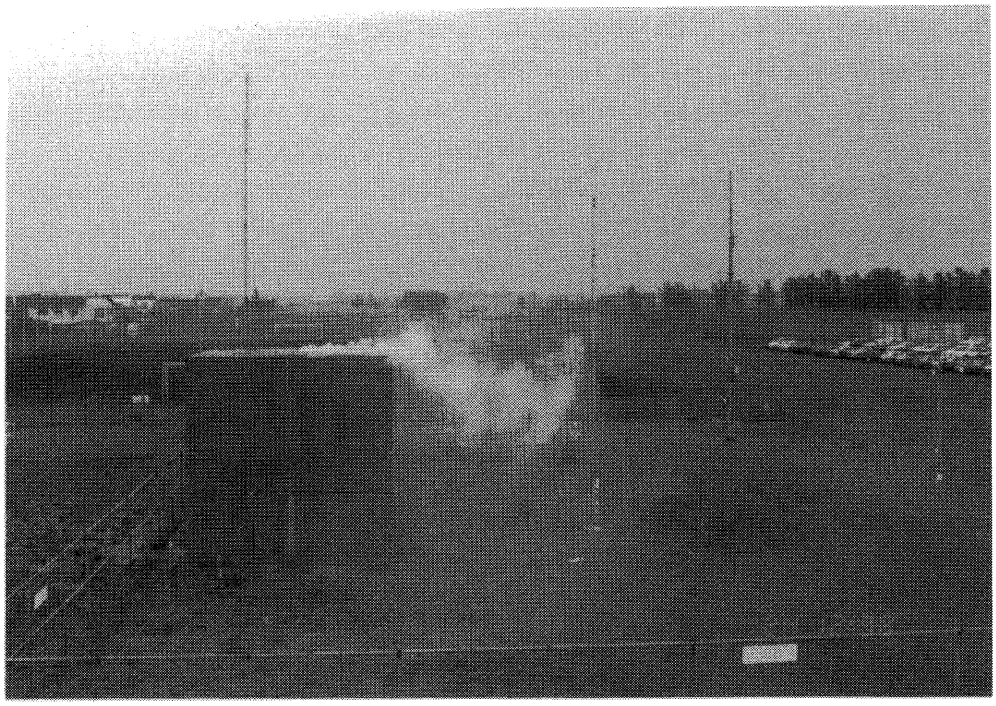

(b)

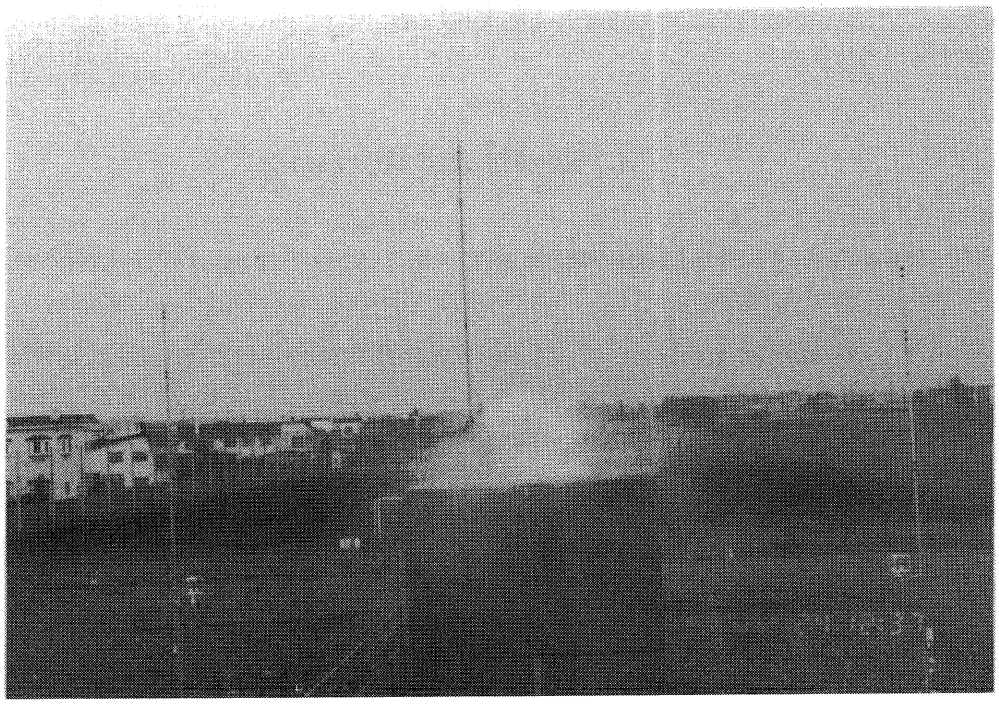

Figure 8. Smoke released from the cube on the centre of the rooftop. The wind blew from the left side of the pictures. (a) smoke on the roof transported directly downwind (b) smoke on the roof transported upwind.

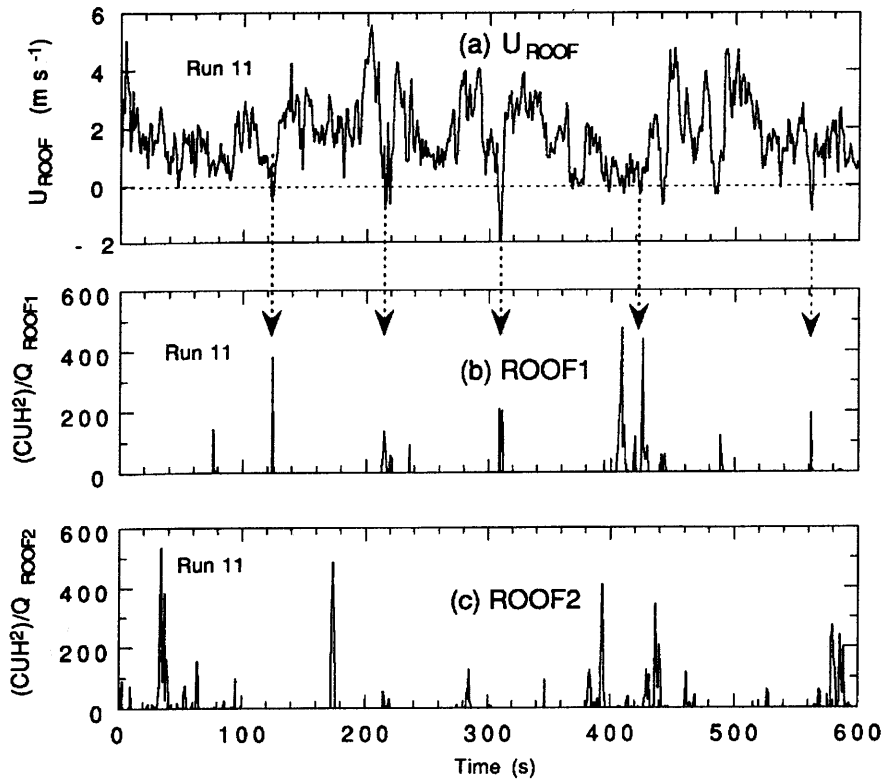

Figure 9. Time series of (a) reverse flow on the roof and (b) normalized concentration fluctuations on the central upwind rooftop location (ROOF1) and (b) normalized concentration fluctuations on the central downwind rooftop location (ROOF2) of Run 11. Negative wind speeds in (a) represent reverse flow on the roof.

turbulence intensity σ_u/U at the model height was extremely high as it was 0.4 or more.

3.2. AVERAGED CONCENTRATION

Figure 4 shows an example of the normalized concentration C^* patterns on the roof. The normalized concentration C^* is given as CUH^2/Q, where C is the measured concentration in ppm, U is the mean oncoming velocity at $z = H$, Q is the emission flow rate. High concentrations were observed both upwind and downwind of the source. Note there was no drastically high concentration region on the roof due to the large turbulence in the suburban area.

Figure 5 illustrates the normalized concentration C^* measured at the central upwind rooftop location (ROOF1) and the downwind location (ROOF2) vs. the turbulence intensity upwind at the model height (z = 5.4 m). The numbers denote field run numbers, and the lines represent wind tunnel data (ϕ = 0°) reported by Ogawa et al. (1983b), in which the effects of four different upwind roughnesses (very smooth to very rough) with σ_u/U from 6.7% (R0 Case) to 26.5% (R6 Case) were investigated. As expected, the value of C^* at both locations upwind and downwind of the source, were lower than the data obtained from wind tunnel

results conducted at moderated turbulence level (R6). This phenomenon might be explained as discussed by Ogawa et al. (1983b). For small turbulence intensity, a reverse flow on the roof occurred, the pollutant was transported upwind and the highest concentrations were measured at the location upwind of the source. When turbulence intensity increased to approximately $\sigma_u/U = 20$–30%, the mean negative wind speed on the roof was not observed, and the high rooftop concentration was observed downwind of the source. In this field study, C^* values were lower than the wind-tunnel data (R6 case). This might be due to the fact that the high turbulence in the suburban area increased the initial plume diffusion on the roof and caused the concentrations downwind of the source to decrease. The oncoming flow condition affects not only the concentration on the roof but also that at ground level.

Figure 6 shows an example of the normalized concentration C^* patterns on the ground. The maximum ground level concentration was observed near the cube. Figure 7 represents the normalized concentration C^* on the central axis of the cube on the ground. Ogawa et al.'s (1983b) wind tunnel data (R6 case; $\phi = 0°$) are also shown in this figure. In comparison to the R6 case and field Run 6 case, C^* is lower and decreased rapidly with increasing distance. Table II shows the turbulence intensity in the field and in the wind tunnel. The vertical components for both the wind tunnel (R6) and field (Run 6) were of the same order, but the values of longitudinal and lateral components of the wind tunnel were lower than those of the field. Both components affected the structure of the cavity and caused a low ground level concentration.

3.3. INSTANTANEOUS CONCENTRATION ON THE ROOF

In the previous section, the averaged levels of concentration were described. The results show that a high concentration was observed at the upwind position, although the mean velocity on the roof was positive. To clarify the phenomena on the roof, a smoke visualization was done and the instantaneous concentrations and velocity were investigated using two fast-response FIDs and an ultrasonic anemometer.

The smoke for the visualization was released from the centre of the roof. Two typical patterns are shown in Figure 8. In Figure 8(a), the smoke on the roof is being transported directly downwind and is trapped in the wake behind the cube. In Figure 8b, on the other hand, the smoke on the roof is being transported upwind from the source and no downdraft phenomenon was observed behind the cube.

Figure 9 presents a time series of the longitudinal velocity at the the roof center and normalized concentrations at the upwind (ROOF1) and the downwind (ROOF2) rooftop locations. The plots were smoothed by a 1-s running average. Negative longitudinal velocity represents reverse flow on the roof. It is clear that when the reverse flow on the roof occurred, the tracer gas was detected at the position upwind of the source (ROOF1). This result indicates that almost all of the gas detected at the upwind position was transported by reverse flow. It is for this

reason that a high concentration was observed at the upwind position (ROOF1), although the average longitudinal velocity on the roof was positive.

4. Summary

Diffusion properties of central rooftop emission from a model cube in a suburban area were observed during a field study performed in Sapporo, Japan. It was found that:

(1) On the roof, high concentrations were observed both upwind and downwind of the source, although the mean velocity U was positive. The field study did not reveal any drastically high concentration regions on the roof due to the large turbulence in the suburban area. The values of normalized concentration at the locations upwind and downwind of the source were lower than those obtained from wind-tunnel data conducted at moderated turbulence levels. At ground level, the mean concentrations along the model centre line show the highest value near the cube and decay rapidly in the downstream direction.

(2) The relationship between the instantaneous concentrations and instantaneous velocity was investigated using two fast-response concentration detectors and an ultrasonic anemometer. It was found that when reverse flow occurred on the roof, the tracer gas was detected upwind of the source.

Acknowledgments

The authors wish to express their thanks to Mr K. Uehara of National Institute for Environmental Studies, Japan and Dr Ohara of Institute of Behavioral Science for their cooperation in the field studies and their discussions. The authors also would like to thank T. Tomabechi, Assistant Professor at the Hokkaido Institute of Technology, for his assistance during this project.

References

Bowne, N. E. and Ball, J. T.: 1970, 'Observational Comparison of Rural and Urban Boundary Layer Turbulence', *J. Appl. Meteorol.* **9**, 862–873.

Counihan, J.: 1971, 'Wind Tunnel Determination of the Roughness Length as a Function of the Fetch and Density of Three-dimensional Roughness Elements', *Atmos. Environ.* **5**, 637–642.

Carl, M. D.,Tarbell,T. C., and Panofsky, H.A.: 1973, 'Profiles of Wind and Temperature from Towers over Homogeneous Terrain', *J. Atmos. Sci.* **30**, 788–794.

Drivas, P. J. and Shair, F. H.: 1974, 'Probing the Air Flow within the Wake Downwind of a Building by Means of a Tracer Technique', *Atmos. Environ.* **8**, 1165–1175.

Halitsky, J.: 1963, 'Gas Diffusion Near Buildings', *ASHRAE Trans.* **69**, 464–485.

Higson, H. L., Griffiths, R. F., Jones, C. D., and Hall, D. J.: 1994, 'Concentration Measurements Around an Isolated Building: A Comparison between Wind Tunnel and Field Data', *Atmos. Environ.* **28**, 1827–1836.

Hinds, W. T.: 1969, 'Peak-to Mean Concentration Ratios from Ground-Level Sources in Building Wakes', *Atmos. Environ.* **3**, 145–156.
Jackson, P. S.: 1978, 'Wind Structure Near a City Center', *Boundary-Layer Meteorol.* **15**, 323–340.
Jones, C. D. and Griffiths, R. F.: 1984, 'Full-Scale Experiments on Dispersion around an Isolated Building Using an Ionized Air Tracer Technique with Very Short Averaging Time', *Atmos. Environ.* **18**, 903–916.
Lettau, H: 1969, 'Note on Aerodynamic Roughness-Parameter Estimation on the Basic of Roughness-Element Description', *J. Appl. Meteorol.* **8**, 828–832.
Munn, R. E. and Cole, A. F. W.: 1967, 'Turbulence and Diffusion in the Wake of a Building', *Atmos. Environ.* **1**, 33–43.
Ogawa, Y. and Oikawa, S.: 1982, 'A Field Investigation of the Flow and Diffusion around a Model Cube', *Atmos. Environ.* **16**, 207–222.
Ogawa, Y., Oikawa, S., and Uehara, K.: 1983a, 'Field and Wind Tunnel Study of the Flow and Diffusion around a Model Cube – I. Flow Measurements', *Atmos. Environ.* **17**, 1145–1159.
Ogawa, Y., Oikawa, S., and Uehara, K.: 1983b, 'Field and Wind Tunnel Study of the Flow and Diffusion around a Model Cube – II. Nearfield and Cube Surface Flow and Concentration Patterns', *Atmos. Environ.* **17**, 1161–1171.
Oikawa, S. and Meng, Y.: 1995, 'Turbulence Characteristics and Organized Motion in a Suburban Roughness Sublayer', *Boundary-Layer Meteorol.* **74**, 289–312.
Rotach, M. W.: 1993, 'Turbulence Close to a Rough Urban Surface. Part I: Reynolds Stress', *Boundary-Layer Meteorol.* **65**, 1–28.
Smith, D. G.: 1975, 'Influence of Meteorological Factors upon Effluents Concentrations on and near Buildings with Short Stacks', *Proc. 68th Annual APCA Meeting*, Paper No. 75-26.2.
Uno, I., Wakamatsu, S., Ueda, H., and Nakamura, A.: 1988, 'An Observational Study of the Structure of the Nocturnal Urban Boundary Layer', *Boundary-Layer Meteorol.* **45**, 59–82.
Wilson, D. J.: 1976, 'Concentration of Air Intakes from Roof Exhaust Vents', *ASHRAE Trans.* **82**, 1024–1038.